Journal of Organometallic Chemistry, 472 (1994) 303–310

Extended normal coordinate analysis of an (arene)osmium(II) complex with the inclusion of the ring ligand *

T. Polzer and W. Kiefer

Institut für Physikalische Chemie der Universität Würzburg, Marcusstr. 9–11, D-97070 Würzburg (Germany)

(Received September 8, 1993)

Abstract

Results are presented of an optimized valence force field of the dihydridoosmium(II) complex [(mes)OsH$_2$(CO)] (mes = C$_6$H$_3$(CH$_3$)$_3$-2,4,6) in which the ring was treated as a point mass. The Raman and IR spectra of metal-coordinated mesitylene are given and the results of normal coordinate analysis of the arene described. From the results, a modified general valence force field including the whole ring ligand has been calculated. The results are discussed, and compared with those of the model with point mass approximation.

Key words: Osmium; Arene; Normal coordinate analysis; Force field; Raman spectroscopy; Infrared spectroscopy

1. Introduction

During our investigation of C–H activation by osmium(II) complexes we have previously studied the vibrational spectroscopy of relevant compounds [1,2]. Information about force constants and bond properties, based on vibrational analysis of the compound, is of great importance for further investigations concerning the selective excitation of certain modes in order to favour C–H activation products. Therefore, we improved the normal coordinate analysis (NCA) presented in ref. 2 by making use of a refined set of structure parameters, and particularly by the inclusion of the ring ligand instead of a point mass approximation (PMA). The PMA is a method often used in vibrational spectroscopy of organometallic compounds, especially if ligands are considered too bulky for calculations or if the bands of only a small part of a molecule, e.g. the modes of the carbonyl groups [3], are known. On the other hand, there are reports of NCA calculations of a complete half sandwich complex [6–8] (although this was a very symmetric one and therefore the NCA was a simplified) where the authors focused on the changes on going from the free and the coordinated ligand. A comparison between the PMA and a complete model calculation has not been reported until now. In view of this and the fact that we now have novel geometry data for the osmium compound, we have undertaken both the point mass approximation and the inclusion of the ring ligand in the NCA of [(mes)OsH$_2$(CO] to derive information on the difference between the two models. A critical comparison between the results for the chosen models is given.

2. Calculations

2.1. Structure parameters

In the recent NCA of [(mes)OsH$_2$(CO)] [2] we had to use geometrical data adapted from similar species, because no accurate structure parameters from X-ray diffraction studies are available. In the present paper, we make use of an energy optimized geometry [9] based on GAUSSIAN 90 calculations [10]. Bond lengths and bond angles used for both models are compiled in Table 1. In comparison to the data used in ref. 2, the Os–C bond length and the distance between the centre of the ring ligand and the metal atom are increased by 12% and 15%, respectively. The bond angles remain nearly unchanged, except that the bond angle H–Os–H is decreased by 11%. Owing to coordination of the ring

---

Correspondence to: Professor W. Kiefer.

* Dedicated to Professor Helmut Werner on the occasion of his 60th birthday.

0022-328X/94/$7.00
SSDI 0022-328X(93)24238-Z

the mean C–C distance within the ring is increased by 10% compared with that in free mesitylene. The symmetry is C_s for the PMA and the complete model.

2.2. *Vibrational force field*

The method of performing the NCA of the complete molecule is similiar to that used for more highly symmetrical or more simple molecules [8,11]. A novel NCA was carried out by treating the ring ligand as a point mass; and then, the force field of free mesitylene [12] was refined using the geometry and the vibrational frequencies of the coordinated ring ligand. Finally, the two force fields were combined and the resulting force field was additionally modified by inclusion of interaction force constants and refinements of the force constants. A direct merge is clearly not possible, because the "one" atom representing the ring ligand in the PMA had to be replaced by the six C-atoms of the mesitylene molecule. This replacement demands a new set-up of the structure of the part of the force field of the $H_2Os(CO)$ unit and fewer interaction force constants with respect to the internal coordinates involving the Os–H bond had to be used. The force fields were set up in internal coordinates without conversion into symmetry coordinates because the symmetry of the molecule is very low, and furthermore we use these force fields as a base for further calculations of Os^{II} complexes. The programs used for the calculations were the same as those described in ref. 2.

In an initial step, we had to repeat the calculations on the point mass approximation, where the mass of the mesitylene ligand is centred in a point mass at the centre of the ring. The resulting force field of ref. 2 could not be adopted directly because the changes in the structural data lead to large errors in the calculated positions of the normal modes which cannot be removed by simple refinement of the force constants. It has been shown [13] that even small changes in the bond length are responsible for such large deviations of the calculated band positions, whereas changes in the bond angles within 10% result in only small errors. Thus, the force field of the molecule had to be modified because of the changed geometry, and some more interaction force constants had to be added with respect to the recent field. The defined internal coordinates are shown in Fig. 1, and the force constants are compiled in Table 2. Observed and calculated frequencies, together with the assignments and potential energy distribution, are listed in Table 3.

TABLE 1. Bond lengths (Å) and bond angles (°) of [(mes)OsH_2(CO)] used as input data for the two models discussed in this paper; M = centre of mesitylene; R = CH_3 group as a point mass

Bond angles			
H–Os–H	80.20	M–Os–C_{ring}	53.87
M–Os–H	135.10	Os–M–C_{ring}	90.00
M–Os–C_{CO}	142.50	Os–C–O	179.00
Bond lengths			
Os–H	1.736	C_{ring}–C_{ring}	1.416
Os–C	2.060	C_{ring}–H	1.068
C–O	1.135	C_{ring}–R	1.505
Os–M	1.939	C_{ring}–Os	2.400

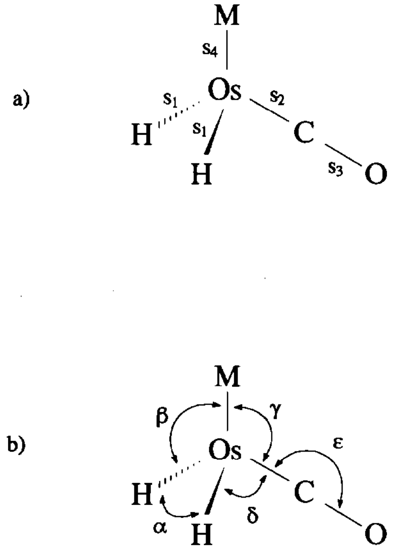

Fig. 1. Internal coordinates of the point mass model of (mes)OsH_2(CO), (a) stretches, (b) bendings.

The next step was to determine the vibrational frequencies of the coordinated mesitylene and to set up its force field. The vibrational spectroscopy of free mesitylene has frequently been investigated [12,14–17] but only a few items of vibrational data for the coordinated arene have been reported up to now [18,19]; moreover, only half-sandwich complexes with metals of Group VI were considered in those papers. We have carried out a vibrational assignment of the coordinated mesitylene based on our Raman and IR measurements and on the current literature data. Figure 2 shows the complete vibrational spectra of [(mes)OsH_2(CO] (including the CH-stretching region) with the assigned modes of the ring ligand. Part of this spectrum (without the CH-stretching region) has already been presented in ref. 2. The vibrational frequencies and assignments of free as well as coordinated mesitylene are listed in Table 4. We were also able to assign the modes of the methyl groups (see Table 5). If the methyl groups of the ring and the rest of the metal fragment are considered as point masses, the symmetry of the ring is lowered from D_{3h} of the free molecule to C_{3v}. Therefore, the assignments are related to the local C_{3v} symmetry. The A_2-modes which are inactive in both the Raman and the IR spectrum of the free ligand become active as a result of the coordination. However, they remain of very weak intensity and their band positions remain uncertain.

TABLE 2. Internal coordinates and calculated force constants of [(mes)OsH$_2$(CO)] with the point mass approximation used in this paper (for definitions see Fig. 1)

Force constant type	Definition	Value [a]
Diagonal		
Os–H stretch	s_1	2.517
Os–C stretch	s_2	4.826
C–O stretch	s_3	13.314
Os–M stretch	s_4	4.979
H–Os–H bend	α	0.320
M–Os–H bend	β	0.369
M–Os–C bend	γ	1.014
C–Os–H bend	δ	0.814
Os–C–O bend	ϵ	1.480
Stretch / stretch interaction		
OsH stretch/OsH stretch	s_1s_1	0.002
OsH stretch/CO stretch	s_1s_3	0.036
OsH stretch/OsM stretch	s_1s_4	0.009
OsC stretch/CO stretch	s_2s_3	−0.077
OsC stretch/OsM stretch	s_2s_4	−0.195
CO stretch/OsM stretch	s_3s_4	0.105
Stretch / bend interaction		
OsH stretch/HOsH bend	$s_1\alpha$	−0.008
OsH stretch/MOsC bend	$s_1\gamma$	0.020
OsH stretch/OsCO bend	$s_1\epsilon$	−0.024
Os stretch/HOsH bend	$s_2\alpha$	0.047
OsC stretch/MOsH bend	$s_2\beta$	0.032
OsC stretch/MOsC bend	$s_2\gamma$	−0.044
OsC stretch/HOsC bend	$s_2\delta$	0.179
OsC stretch/OsCO bend	$s_2\epsilon$	0.172
CO stretch/MOsC bend	$s_3\gamma$	−0.079
OsM stretch/HOsH bend	$s_4\alpha$	0.015
OsM stretch/MOsH bend	$s_4\beta$	0.179
OsM stretch/MOsC bend	$s_4\gamma$	0.063
OsM stretch/HOsC bend	$s_4\delta$	−0.024
OsM stretch/OSCO bend	$s_4\epsilon$	−0.043
Bend / bend interaction		
HOsH bend/MOsH bend	$\alpha\beta$	0.113
HOsH bend/MOsC bend	$\alpha\gamma$	0.007
HOsH bend/HOsC bend	$\alpha\delta$	−0.036
HOsH bend/OsCO bend	$\alpha\epsilon$	0.074
H$_1$OsM bend/H$_2$OsM bend	$\beta\beta$	0.228
HOsM bend/MOsC bend	$\beta\gamma$	0.068
HOsM bend/HOsC bend	$\beta_1\delta_1/\beta_2\delta_2$	0.120
HOsM bend/HOsC bend	$\beta_1\delta_2/\beta_2\delta_1$	−0.068
HOsM bend/OsCO bend	$\beta\epsilon$	0.021
MOsC bend/HOsC bend	$\gamma\delta$	0.022
MOsC bend/OsCO bend	$\gamma\epsilon$	0.156
H$_1$OsC bend/H$_2$OsC bend	$\delta\delta$	−0.299

[a] Values for stretches and their interactions are in mdyn Å^{-1}, for bendings, waggings and torsions and all interactions thereoff in mdyn Å rad^{-2} and for interactions of stretches with bendings, waggings and torsions mdyn rad^{-1}.

TABLE 3. Observed and calculated wavenumbers for [(mes)OsH$_2$(CO)] within the point mass approximation

Observed (cm^{-1}) [a]	Calculated (cm^{-1})	Assignment	PED (%) [b]
2066	2066	ν_s(Os–H)	100s_1
2062	2062	ν_{as}(Os–H)	100s_1
1936	1936	ν(C–O)	87s_3 + 13s_2
810	810	δ(C–Os–H)	50ϵ + 37δ + 8β
733	733	τ(H–Os–H)	79δ + 21β
605	605	ω(H–Os–H)	42δ + 33ϵ + 21β
558	558	δ(H–Os–H)	86α + 9β
546	546	ν(Os–C)	79s_2 + 12s_3
329	329	ν(Os–M)	95s_4 + 4s_2
166	166	δ(M–Os–H)	98β
137	137	δ(M–Os–C)	78γ + 11δ + 6β

[a] Ref. 2. [b] Potential energy distribution (PED) values below 5% are omitted.

The last step in our theoretical treatment was the calculation for the complete molecule. We used the previously investigated force field for free mesitylene [12] and refined it on the basis of the changed band positions. The methyl groups do not couple to any significant extent with the ring, and they are considered as point masses with $m = 15$ at the positions of the C-atoms. A limitation of the model is the fact that we had to use fixed positions of the atoms despite the known rotation of the ring around the z-axis of the molecule at room temperature. Because of the overall C_s symmetry of the molecule, the atom groups of the ring ligand are no longer undistinguishable (*i.e.* viewed from the carbonyl group). We took this into account by using separate off-diagonal constants that describe the different interactions of the various ligand atoms, whereas the part of the force field describing the ring ligand was kept symmetrical. The defined internal coordinates are shown in Fig. 3, and they are also given together with the calculated force constants in Table 6. The observed and calculated frequencies of [(mes)-OsH$_2$(CO)] together with assignments and PED are finally compiled in Table 7.

3. Discussion

As can be seen in Table 3, there is excellent agreement between the calculated and observed frequencies for the PMA model. The five stretch and six deformation modes were calculated with an average error of 0.013% by use of a force field with 12 diagonal elements and 51 off-diagonal elements represented by 44 force constants. The vibrational assignment made in ref. 2 is unchanged, and the resulting PED does not differ very much from that reported there. When the ring ligand is included instead of the PMA, the force field for the complete molecule can be calculated under the conditions mentioned above with a set of 65 diagonal elements and 462 off-diagonal elements represented by a total of 100 force constants. The calculated frequencies agree very well with the measured values with deviations of < 4 cm^{-1}.

The in-plane modes of the ring are hardly coupled with other modes of the molecule. This is easily explained by the fact that the displacement vectors of the in-plane coordinates are almost perpendicular to the Os–C$_{ring}$ bond axis. Furthermore, the large mass of the osmium atom screens them from the residual ligands. Most of the in-plane band positions are only slightly changed except for the C–H stretching modes and the two C–C stretching modes of E type symmetry in the region from 1400 cm^{-1} to 1600 cm^{-1}. It was recently reported [18,20,21] that the C–H stretching modes of an aromatic ring could be shifted to higher wavenumbers upon coordination, and thus the corresponding force constant s_2 is enlarged slightly. One E type mode is raised from 1383 cm^{-1} to 1455 cm^{-1} and the other is lowered from 1610 cm^{-1} to 1522 cm^{-1}. The calculation shows that, compared with the free mesitylene, the increase in the C–C stretch force constant s_6 and a decrease in the interaction force constant $\eta\eta$ are mainly responsible for the shift.

In the case of the out-of-plane modes, the situation is completely different. The mentioned displacements

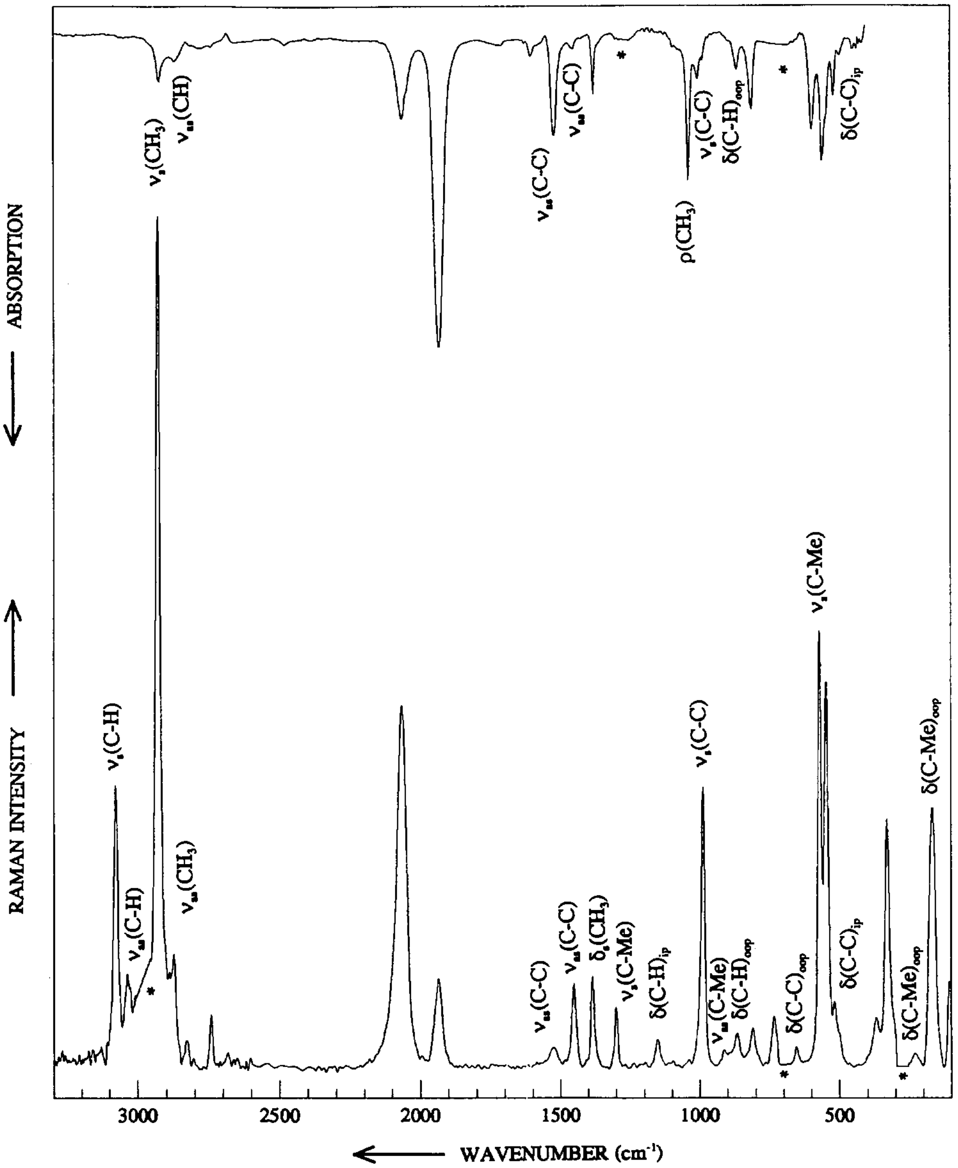

Fig. 2. Raman and IR spectra of [(mes)OsH$_2$(CO)] in CH$_2$Cl$_2$; * marks the position of solvens compensation. For experimental details see ref. 2.

TABLE 4. Assignments and band positions of the normal modes of free mesitylene and coordinated at [(mes)OsH$_2$(CO)] with respect to local symmetry of the ring

Free mesitylene (D_{3h}) [a]			Coordinated mesitylene (C_{3v})		
Symmetry	Band	Position (cm^{-1})	Symmetry	Band	Position (cm^{-1})
E'_1	ν_{as}(CH)	3027	A_1	ν_s(C–H)	3078
A'_1	ν_s(CH)	3006	E	ν_{as}(C–H)	3034
E'_1	ν_{as}(C–C)	1610	E	ν_{as}(C–C)	1522
E	ν_{as}(C–C)	1382	E	ν_{as}(C–C)	1455
A'_2	δ(C–H)$_{ip}$	(1290–1460) [b]	A_2	δ(C–H)$_{ip}$	1451 [d]
A'_1	ν_s(C–Me)	1301	A_1	ν_s(C–Me)	1299
A'_2	δ(C–C)$_{ip}$	(1200–1250) [b]	A_2	δ(C–C)$_{ip}$	1222 [d]
E'	δ(C–H)$_{ip}$	1166	E	δ(C–H)$_{ip}$	1152
A'_1	ν_s(C–C)	998	A_1	ν_s(C–C)	989
E'	ν_{as}(C–Me)	929	E	ν_{as}(C–Me)	913
E''	δ(C–H)$_{oop}$	881	E	δ(C–H)$_{oop}$	878
A''_2	δ(C–H)$_{oop}$	837	A_1	δ(C–H)$_{oop}$	826
A''_2	δ(C–C)$_{oop}$	688	A_1	δ(C–C)$_{oop}$	669
A'_1	ν_s(C–Me)	578	A_1	ν_s(C–Me)	570
E''	δ(C–C)$_{oop}$	(430–540) [c]	E	δ(C–C)$_{oop}$	565 [d]
E'	δ(C–C)$_{ip}$	515	E	δ(C–C)$_{ip}$	517
A'_2	δ(C–Me)$_{ip}$	(300–500) [b]	A_2	δ(C–Me)$_{ip}$	324 [d]
E'	δ(C–Me)$_{ip}$	275	E	δ(C–Me)$_{ip}$	275
E''	δ(C–Me)$_{oop}$	225	E	δ(C–Me)$_{oop}$	225
A''_2	δ(C–Me)$_{oop}$	183	A_1	δ(C–Me)$_{oop}$	173

[a] Refs. 12, 14–17. [b] Not active in both Raman and infrared spectroscopy. [c] Position is uncertain due to very low intensity. [d] Calculated (see Table 5).

coincide with those of the Os–C$_{ring}$ coordinates and strong coupling occurs. The two different modes with E symmetry are caused by the ligands, which produce a different environment for each mode. Thus, the E type bands in particular are split in the calculation. The reported values as given in Table 6 are the average of the two split modes.

The question to be answered was whether treatment of the ring as a point mass is a useful approximation. We obtained a force constant for the Os–C$_{ring}$ stretch coordinate of 1.211 mdyn/Å. The value of the force constant of the Os–M stretch coordinated was calculated to be 4.979 mdyn/Å. Simply related to one single Os–C$_{ring}$ bond this would be 0.830 mdyn/Å, which means a difference of about 30% compared with 1.211 mdyn/Å. This is similar to the other internal coordinates involving the ring ligand, in which large changes of their force constants occur. On the other hand,

TABLE 5. Band positions of the modes of the methyl groups of the coordinated mesitylene of [(mes)OsH$_2$(CO)]

Raman (cm^{-1})	IR (cm^{-1})	Assignment
2919vs, p	2920w	ν_s(CH$_3$)
2872m	2875vw	ν_{as}(CH$_3$)
1442w, sh	1440w	δ_{as}(CH$_3$)
1385m	1383m	δ_s(CH$_3$)
1036w	1040s	ρ(CH$_3$)

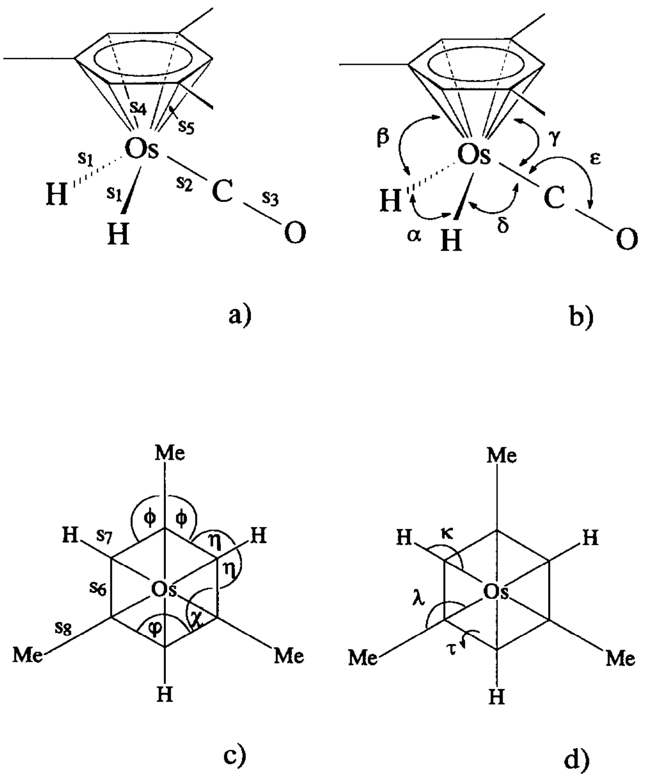

Fig. 3. Internal coordinates for [(mes)OsH$_2$(CO)], (a) stretches for the H$_2$Os(CO) unit, (b) bendings for the H$_2$Os(CO) unit, (c) stretches and in-plane bendings of the ring, (d) out-of-plane bendings and torsions of the ring.

TABLE 6. Internal coordinates and force constants of [(mes)-$OsH_2(CO)$] without point mass approximation (PED) (for definitions see Fig. 3)

Force constant type	Definition	Value
Diagonal		
Os-H stretch	s_1	2.497
Os-C_{CO} stretch	s_2	4.792
C-O stretch	s_3	13.419
Os-$C_{ring/H}$ stretch	s_4	1.211
Os-$C_{ring/Me}$ stretch	s_5	1.211
C-C stretch	s_6	6.777
C-H stretch	s_7	4.028
C-Me stretch	s_8	4.530
H-Os-H bend	α	0.285
C_{ring}-Os-H bend	β	0.185
C_{ring}-Os-C_{CO} bend	γ	2.013
C_{CO}-Os-H bend	δ	0.810
Os-C-O bend	ϵ	1.217
C-C_H-C bend i.p.	ϕ	0.677
C-C_{Me}-C bend i.p.	χ	1.742
C-C-H i.p.	η	0.777
C-C-Me i.p.	φ	1.408
C-H bend o.o.p.	κ	0.085
C-Me bend o.o.p.	λ	0.374
C-C torsion	τ	0.415
H-C-Os bend	μ	0.035
Me-C-Os bend	π	0.168
Stretch / stretch interaction		
Os-H stretch/Os-H stretch	s_1s_1	0.002
Os-C_{CO} stretch/C-O stretch	s_2s_3	−0.001
Os-$C_{ring/H}$ stretch/Os-$C_{ring/H}$ stretch	s_4s_4	−0.184
Os-$C_{ring/Me}$ stretch/Os-$C_{ring/Me}$ stretch	s_5s_5	−0.184
Os-$C_{ring/H}$ stretch/C-O stretch	s_4s_6	−0.050
Os-$C_{ring/Me}$ stretch/C-O stretch	s_5s_6	−0.050
Os-$C_{ring/H}$ stretch/C-H stretch	s_4s_7	−0.009
Os-$C_{ring/Me}$ stretch/C-Me stretch (adjacent)	s_5s_8'	0.008
Os-$C_{ring/Me}$ stretch/C-Me stretch (1 adjacent)	s_5s_8''	−0.015
C-C stretch/C-C stretch (adjacent)	s_6s_6'	1.788
C-C stretch/C-C stretch (1 adjacent)	s_6s_6''	0.639
C-C stretch/C-H stretch	s_6s_7	−1.986
C-C stretch/C-Me stretch	s_6s_8	0.127
C-H stretch/C-H stretch	s_7s_7	0.160
C-H stretch/C-Me stretch	s_7s_8	0.7047
C-Me stretch/C-Me stretch	s_8s_8	−0.333
Stretch / bend interaction		
Os-C_{CO} stretch/C_{CO}-Os-H bend	$s_2\delta$	0.047
Os-C_{CO} stretch/H-C-Os bend	$s_2\mu$	0.032
Os-C_{CO} stretch/Me-C-Os bend	$s_2\pi$	−0.014
C-O stretch/C_{CO}-Os-H bend	$s_3\delta$	0.001
C-O stretch/Os-C-O bend	$s_3\epsilon$	0.009
Os-$C_{ring/H}$ /C_{ring}-Os-H bend	$s_4\gamma$	−0.132
Os-$C_{ring/H}$ /C-C_H-C bend i.p.	$s_4\phi$	−0.055
Os-$C_{ring/H}$ /C-C_{Me}-C bend i.p.	$s_4\chi$	0.044
Os-$C_{ring/H}$ /C-C-H i.p.	$s_4\eta$	−0.137
Os-$C_{ring/H}$ /C-C-Me i.p.	$s_4\varphi$	−0.275
Os-$C_{ring/H}$ /C-H bend o.o.p	$s_4\kappa$	−0.130
Os-$C_{ring/Me}$ /C_{ring}-Os-H bend	$s_5\beta$	0.047
Os-$C_{ring/Me}$ /C_{ring}-Os-C_{CO} bend	$s_5\gamma$	0.004
Os-$C_{ring/Me}$ /C-C_H-C bend i.p.	$s_5\phi$	0.013
Os-$C_{ring/Me}$ /C-C_{Me}-C bend i.p.	$s_5\chi$	−0.039
Os-$C_{ring/Me}$ /C-C-H bend i.p.	$s_5\eta$	0.0124
Os-$C_{ring/Me}$ /C-C-Me bend i.p.	$s_5\varphi$	−0.023
Os-$C_{ring/Me}$ /C-Me bend o.o.p.	$s_5\lambda$	0.004
C-C stretch/C-C_H-C bend i.p.	$s_6\phi$	−0.486
C-C stretch/C-C_{Me}-C bend i.p.	$s_6\chi$	0.319
C-C stretch/C-C-H bend i.p.	$s_6\eta$	0.404
C-C stretch/C-C-Me bend i.p.	$s_6\varphi$	−0.408
C-H stretch/C-C_H-C bend i.p.	$s_7\phi$	−1.124
C-H stretch/C-C_{Me}-C bend i.p.	$s_7\chi$	0.037
C-H stretch/C-C-H bend i.p.	$s_7\eta$	−0.139
C-H stretch/C-C-Me bend i.p.	$s_7\varphi$	0.940
C-Me stretch/C-C_H-C bend i.p.	$s_8\phi$	−0.003
C-Me stretch/C-C_{Me}-C bend i.p.	$s_8\chi$	−0.019
C-Me stretch/C-C-H bend i.p.	$s_8\eta$	−0.007
C-Me stretch/C-C-Me bend i.p.	$s_8\varphi$	0.794
Bend / bend interaction		
H-Os-H bend/C_{CO}-Os-H bend	$\alpha\delta$	−0.012
H-Os-H bend/Os-C-O bend	$\alpha\epsilon$	0.021
C_{ring}-Os-H bend/C_{ring}-Os-H bend	$\beta\beta$	−0.030
C_{ring}-Os-H bend/C_{ring}-Os-C bend	$\beta\gamma$	−0.620
C_{ring}-Os-H bend/C_{CO}-Os-H bend	$\beta\delta$	0.035
C_{CO}-Os-H bend/C_{CO}-Os-H bend	$\delta\delta$	−0.006
C_{CO}-Os-H bend/Os-C-O bend	$\delta\epsilon$	0.025
C-C_H-C bend i.p./C-C_H-C bend i.p.	$\phi\phi$	−0.345
C-C_H-C bend i.p./C-C_{Me}-C bend i.p.	$\phi\chi$	0.501
C-C_H-C bend i.p./C-C-H bend i.p.	$\phi\eta$	−0.057
C-C_H-C bend i.p./C-C-Me bend i.p.	$\phi\varphi$	−0.019
C-C_{Me}-C bend i.p./C-C_{Me}-C bend i.p.	$\chi\chi$	0.227
C-C_{Me}-C bend i.p./C-C-H bend i.p.	$\chi\eta$	−0.168
C-C-H bend i.p./C-C-H bend i.p.	$\eta\eta$	0.150
C-C-H bend i.p./C-C-Me bend i.p.	$\eta\varphi$	−0.063
C-C_{Me}-C bend i.p./C-C-Me bend i.p.	$\chi\varphi$	0.077
C-C-Me bend i.p./C-C-Me bend i.p.	$\varphi\varphi$	0.510
C-H bend o.o.p./C-H bend o.o.p.	$\kappa\kappa$	0.003
C-H bend o.o.p./C-Me o.o.p.	$\kappa\lambda$	−0.002
C-H bend o.o.p./C-C torsion	$\kappa\tau$	−0.005
C-H bend o.o.p./H-C-Os bend	$\kappa\mu$	−0.006
C-Me o.o.p./C-Me o.o.p.	$\lambda\lambda$	−0.034
C-Me o.o.p./C-C torsion	$\lambda\tau$	0.225
C-Me o.o.p./Me-C-Os bend	$\lambda\pi$	−0.031
C-C torsion/C-C torsion (adjacent)	$\tau\tau$	0.012
C-C torsion/C-C torsion (1 adjacent)	$\tau\tau'$	0.021
C-C torsion/C-C torsion (2 adjacent)	$\tau\tau''$	−0.003
H-C-Os bend/H-C-Os bend	$\mu\mu$	0.099
H-C-Os bend/Me-C-Os bend	$\mu\pi$	0.053
Me-C-Os bend/Me-C-Os bend	$\pi\pi$	0.009

there are only small differences in the force constants of the internal coordinates of the $H_2Os(CO)$ unit between the PMA and the complete calculation.

Hence, it follows that the point mass approximation in a NCA of a half-sandwich complex with "piano stool" geometry and with a heavy centre atom and other relatively light ligands also yields useful results. Only the force constants of the point mass itself have to be considered critically.

TABLE 7. Observed and calculated wavenumbers for [(mes)OsH$_2$(CO)] and potential energy distribution (PED) (for internal coordinates see Fig. 2)

Observed (cm^{-1})	Calculated (cm^{-1})	Assignment	PED (%) [a]
3078	3078	ν_s(C–H)	$96s_7$
3034	3034	ν_{as}(C–H)	$88s_7 + 8s_6$
2066	2066	ν_s(Os–H)	$100s_1$
2062	2062	ν_{as}(Os–H)	$100s_1$
1936	1936	ν(C–O)	$88s_3 + 12s_2$
1522	1522	ν_{as}(C–H)	$88\eta + 7s_6$
1455	1455	ν_{as}(C–C)	$46s_6 + 16s_7 + 10\varphi + 9s_8 + 9\chi + 5\eta$
–	1451	δ(C–C)$_{ip}$	$80s_6 + 13\eta + 7\varphi$
1299	1300	ν_s(C–C)	$36\chi + 14\phi + 14\varphi + 11s_6 + 8\eta + 7s_7 + 6s_8$
–	1222	δ(C–H)$_{ip}$	$75\eta + 25s_6$
1152	1153	δ(C–C)$_{ip}$	$48s_6 + 24s_7 + 14s_8 + 6\varphi + 5\chi$
989	990	ν_s(C–C)	$34s_8 + 25s_7 + 23s_6 + 8\chi$
913	913	ν_{as}(C–Me)	$43s_8 + 39s_6 + 9s_7$
878	881	δ(C–H)$_{oop}$	$35\tau + 16s_8 + 16\kappa + 12\lambda + 8s_6 + 5\mu$
826	827	δ(C–H)$_{oop}$	$74\tau + 15\kappa + 8\mu$
810	809	δ(C–Os–H)	$53\delta + 26\epsilon + 8\beta + 5\alpha$
733	730	τ(H–Os–H)	$87\delta + 13\beta$
669	672	δ(C–C)$_{oop}$	$56\lambda + 18\kappa + 8s_4 + 8s_5$
605	604	ω(H–Os–H)	$40\alpha + 30\epsilon + 9\beta + 6\lambda$
570	568	ν_s(C–Me)	$66s_8 + 16s_6 + 8\chi$
–	565	δ(C–C)$_{oop}$	$23\tau + 20\lambda + 7\kappa + 7s_4 + 7s_5 + 6s_6 + 5\chi$
558	559	δ(H–Os–H)	$32\epsilon + 31\delta + 13\alpha + 5\lambda + 5\tau$
546	546	ν(Os–C$_{CO}$)	$86s_2 + 12s_3$
512	512	δ(C–C)$_{ip}$	$28s_6 + 19\chi + 15s_7 + 11\varphi + 7\lambda + 6\tau$
368	367	ν_{as}(Os–ring)	$28s_4 + 28s_5 + 13\tau + 10\kappa + 6\eta + 5\lambda$
329	329	ν_s(Os–ring)	$42s_4 + 42s_5 + 9\kappa$
–	324	δ(C–Me)$_{ip}$	100φ
275	274	δ(C–Me)$_{ip}$	$66\varphi + 21s_7$
225	226	δ(C–Me)$_{oop}$	$36\tau + 18\pi + 13\kappa + 13s_4 + 13s_5$
173	173	δ(C–Me)$_{oop}$	$23\tau + 18s_4 + 18s_5 + 15\pi + 14\lambda + 11\kappa$
166	163	δ(ring–Os–H)	$76\beta + 13\varphi + 11\delta$
137	137	δ(ring–Os–C$_{CO}$)	$23\tau + 20\gamma + 10\mu + 9\kappa + 7s_4 + 7s_5 + 5\alpha + 5\delta$

[a] PED values below 5% are omitted.

Acknowledgements

We gratefully acknowledge support from the Deutsche Forschungsgemeinschaft (SFB 347, Teilprojekt C-2) as well as from the Fonds der Chemischen Industrie. Fruitful collaborations with Dr. U. Wecker and Prof. H. Werner are highly acknowledged. We also thank Dr. B. Warmuth for her GAUSSIAN-90 calculations.

References

1 T. Polzer, U. Posset, C. Engert, V. Deckert and W. Kiefer, in H. Werner, A.G. Griesbeck, W. Adam, G. Bringmann and W. Kiefer (eds.), *Selective Reactions of Metal Activated Molecules*, Vieweg Verlag, Braunschweig, 1992, p. 225.
2 T. Polzer, A. Ellebracht, W. Kiefer, U. Wecker and H. Werner, *J. Organomet. Chem., 438* (1992) 319.
3 F.A. Cotton, *Inorg. Chem., 3* (1964) 702.
4 W.A. Herrmann, A. Kiprof, K. Rydal, J. Tremmel, R. Blom,

R. Alberto, J. Brehm, R.W. Albach, H. Bock, B. Solouki, J. Mink, D. Lichtenberger and N. Gruhn, *J. Am. Chem. Soc.*, *113* (1991) 6527.

5 F.T. Delbeke, E.G. Claeys, G.P. van der Kelen and Z. Eeckhaut, *J. Organomet. Chem.*, *25* (1970) 213.

6 D.C. Andrews, G. Davidson and D.A. Duce, *J. Organomet. Chem.*, *101* (1975) 113.

7 D.M. Adams, R.E. Christopher and D.C. Stevens, *Inorg. Chem.*, *14* (1975) 1562.

8 E.M. Bisby, G. Davidson and D.A. Duce, *J. Organomet. Chem.*, *48* (1978) 93.

9 B. Warmuth, Ph.D. thesis, University of Würzburg 1993.

10 M.J. Frisch, M. Head-Gordon, G.W. Trucks, J.B. Foresman, H.B. Schlegel, K. Raghavachari, M. Robb, J.S. Binkley, C. Gonzalez, D.J. Defrees, D.J. Fox, R.A. Whiteside, R. Seeger, C.F. Melius, J. Baker, R.L. Martin, L.R. Kahn, J.J.P. Stewart, S. Topiol and J.A. Pople, GAUSSIAN 90, Revision J, Gaussian Inc., Pittsburgh, PA, 1990.

11 S. Kjelstrup, S.J. Cyvin, J. Brunvoll and L. Schäfer, *J. Organomet. Chem.*, *36* (1972) 137.

12 T. Polzer and W. Kiefer, in preparation.

13 A. Ellebracht, diploma thesis, University of Würzburg, 1992.

14 J.H.S. Green, D.J. Harrison and W. Kynaston, *Spectrochim. Acta*, *27A* (1971) 793.

15 C. La Lau and R.G. Snyder, *Spectrochim. Acta*, *27A* (1971) 2073.

16 J. Favrot and M.T. Forel, *Can. J. Spectrosc.*, *21* (1976) 144.

17 J.A. Draeger, *Spectrochim. Acta*, *41A* (1985) 607.

18 G. Davidson and E.M. Riley, *J. Organomet. Chem.*, *19* (1969) 101.

19 R.S. Armstrong, M.J. Aroney, C.M. Barnes and K.W. Nugent, *Appl. Organomet. Chem.*, *4* (1990) 569.

20 L. Phillips, A.R. Lacey and M.K. Cooper, *J. Chem. Soc., Dalton Trans.*, (1988) 1383.

21 V.T. Aleksanyan, B.V. Lokshin, G.K. Borisov, G.G. Devyatykh, A.S. Smirnov, R.V. Nazarova, J.A. Koningstein and B.F. Gächter, *J. Organomet. Chem.*, *124* (1977) 293.